PHYSICAL REVIEW D **90,** 014009 (2014)

Mass spectra and decay properties of D_s meson in a relativistic Dirac formalism

Manan Shah,[1,2,*] Bhavin Patel,[2,†] and P. C. Vinodkumar[1,‡]

[1]*Department of Physics, Sardar Patel University, Vallabh Vidyanagar 388120, India*
[2]*P. D. Patel Institute of Applied Sciences, CHARUSAT, Changa 388421, India*

(Received 17 February 2014; revised manuscript received 7 May 2014; published 7 July 2014)

The mass spectra of the D_s meson is obtained in the framework of the relativistic independent quark model using a Martin-like potential for the quark confinement. The predicted excited states are in good agreement with the experimental results as well as with the lattice and other theoretical predictions. The spectroscopic parameters are employed further to compute the decay constant, electromagnetic transition and leptonic decay widths. The present result for its decay constant, f_P (252.82 MeV) is in excellent agreement with the value 252.6 ± 11.1 MeV reported by CLEO-c. The predicted branching ratios for $(D_s \to \tau\bar{\nu}_\tau, \mu\bar{\nu}_\mu)$ $(5.706 \times 10^{-2}, 5.812 \times 10^{-3})$ are in close agreement with the values $[(5.43 \pm 0.31) \times 10^{-2}, (5.90 \pm 0.33) \times 10^{-3}]$ reported in Particle Data Group. The Cabibbo favored semileptonic branching ratio of $[D_s \to \phi e^+ \nu_e (2.01\%)]$ and that of the hadronic decay $[D_s \to \phi\pi^+ (4.62\%)]$ are in very good agreement with the respective Particle Data Group values, and the branching ratio $[D_s \to K^0\pi^+ (2.16 \times 10^{-3})]$ is in very good agreement with the branching ratio of $(2.40 \pm 0.18) \times 10^{-3}$ reported by Belle collaboration.

DOI: 10.1103/PhysRevD.90.014009 PACS numbers: 14.40.Lb, 13.20.-v, 13.20.Gd

I. INTRODUCTION

Having played a major role in the foundation of QCD, heavy hadron spectroscopy has witnessed in the past few years a renewal of interest due to many new states observed in recent years. The remarkable progress at the experimental [1] side, with various high energy machines at *BABAR*, BELLE, BES-III, B-factories, Tevatron, ARGUS collaborations, CLEO, CDF, SELEX, DØ etc., for the study of hadrons has opened up new challenges in the theoretical understanding of hadrons containing one or more heavy flavor quarks. Many of the newly discovered states in the heavy flavor sector do not really fit into our understanding of the conventional mesons. Thus, understanding the structure of these exotic states, particularly the new states $Z_c(3900)$ [2], $Y(4260)$ [2] etc. above the DK (D^*K) threshold attracted considerable interest in the field of hadron spectroscopy very recently. Apart from the challenges posed by the exotics, there are also many states which are the radial and orbital excited states of the known hadrons or admixtures of their nearby states. Particularly, the discoveries of new resonances of D_s states such as $D_s(2638)$ [3], $D_s(2710)$ [4], $D_s(2860)$ [5], $D_s(3040)$ [5] etc., have further generated considerable interest towards the spectroscopy of this double open flavor mesons. Study of the D_s meson carries special interest as it is a hadron with two open flavors $(c, \bar{s})$ that restricts its decay via strong interactions. These particles thus provide us a clean laboratory to study electromagnetic and weak interactions. The masses of low-lying $1S$ and $1P_J$ states of D_s mesons are recorded both experimentally [1] and theoretically [6–15]. However, the existing results on excited heavy-light mesons are partially inconclusive and even contradictory in several cases.

Thus, any attempts towards the understanding of these newly observed states become very important for better understanding the quark-antiquark dynamics within the $Q\bar{q}$ bound state. So, a successful theoretical model can provide important information about the quark-antiquark interactions and the behavior of QCD within the doubly open flavor hadronic system. Though there exist many theoretical models [6–9] to study the hadron properties based on its quark structure, the predictions for low-lying states are off by 60–90 MeV with respect to the respective experimental values. Moreover, the issues related to the hyperfine and fine structure splitting of the mesonic states; their intricate dependence with the constituent quark masses and the running strong coupling constant are still unresolved. Though the validity of nonrelativistic models is very well established and significantly successful for the description of heavy quarkonia, disparities exist in the description of meson containing light flavor quarks or antiquarks.

Apart from the successful predictions of the mass spectra, validity of any phenomenological model depends also on the successful predictions of their decay properties. For better predictions of the decay widths, many models have incorporated additional contributions such as radiative and higher order QCD corrections [14,16–19]. Thus, in this paper we make an attempt to study properties like mass spectrum, decay constants and other decay properties of the

*mnshah09@gmail.com
†azadpatel2003@gmail.com
‡p.c.vinodkumar@gmail.com

D_s meson based on a relativistic Dirac formalism. We investigate the heavy-light mass spectra of the $D_s(c\bar{s})$ meson in this framework with Martin-like confinement potential.

Along with the mass spectra, the pseudoscalar decay constants of the heavy-light mesons have also been estimated in the context of many QCD-motivated approximations. The predictions of such methods cover a wide range of values [20,21]. It is important to have a reliable estimate of the decay constant as it is an important parameter in many weak processes such as quark mixing, CP violation, etc. The leptonic decay of charged meson is another important annihilation channel through the exchange of the virtual W boson. Though this annihilation process is rare, they have clear experimental signatures due to the presence of highly energetic leptons in the final state. There exist experimental observations of the leptonic decays of D_s meson. The leptonic decays of mesons entail an appropriate representation of the initial state of the decaying vector mesons in terms of the constituent quark and antiquark with their respective momenta and spin. The bound constituent quark and antiquark inside the meson are in definite energy states having no definite momenta. However, one can find out the momentum distribution amplitude for the constituent quark and antiquark inside the meson immediately before their annihilation to a lepton pair. Thus, it is appropriate to compute the leptonic branching ratio here and compare our result with the experimental values as well as with the predictions based on other models.

II. THEORETICAL FRAMEWORK

The quark confining interaction of meson is considered to be produced by the nonperturbative multigluon mechanism and this mechanism is unfeasible to estimate theoretically from first principles of QCD. On the other hand, there exists ample experimental support for the quark structure of hadrons. This is the origin of phenomenological models which are proposed to understand the properties of hadrons and quark dynamics at the hadronic scale. In this context for the present study, we assume that the constituent quarks inside a meson are independently confined by an average potential of the form [22]

$$V(r) = \frac{1}{2}(1+\gamma_0)(\lambda r^{0.1} + V_0). \tag{1}$$

To first approximation, the confining part of the interaction is believed to provide the zeroth-order quark dynamics inside the meson through the quark Lagrangian density,

$$\mathcal{L}_q^0(x) = \bar{\psi}_q(x)\left[\frac{i}{2}\gamma^\mu\vec{\partial}_\mu - V(r) - m_q\right]\psi_q(x). \tag{2}$$

In the stationary case, the spatial part of the quark wave functions $\psi(\vec{r})$ satisfies the Dirac equation given by

$$[\gamma^0 E_q - \vec{\gamma}\,\vec{P} - m_q - V(r)]\psi_q(\vec{r}) = 0. \tag{3}$$

The solution of the Dirac equation can be written in two component (positive and negative energies in the zeroth order) form as

$$\psi_{nlj}(r) = \begin{pmatrix} \psi_{nlj}^{(+)} \\ \psi_{nlj}^{(-)} \end{pmatrix}, \tag{4}$$

where

$$\psi_{nlj}^{(+)}(\vec{r}) = N_{nlj}\begin{pmatrix} ig(r)/r \\ (\sigma\hat{r})f(r)/r \end{pmatrix}\mathcal{Y}_{ljm}(\hat{r}), \tag{5}$$

$$\psi_{nlj}^{(-)}(\vec{r}) = N_{nlj}\begin{pmatrix} i(\sigma\hat{r})f(r)/r \\ g(r)/r \end{pmatrix}(-1)^{j+m_j-l}\mathcal{Y}_{ljm}(\hat{r}) \tag{6}$$

and N_{nlj} is the overall normalization constant. The normalized spin angular part is expressed as

$$\mathcal{Y}_{ljm}(\hat{r}) = \sum_{m_l,m_s}\left\langle l, m_l, \frac{1}{2}, m_s | j, m_j \right\rangle Y_l^{m_l}\chi_{\frac{1}{2}}^{m_s}. \tag{7}$$

Here the spinor $\chi_{\frac{1}{2}m_s}$ are eigenfunctions of the spin operators,

$$\chi_{\frac{1}{2}\frac{1}{2}} = \begin{pmatrix} 1 \\ 0 \end{pmatrix}, \qquad \chi_{\frac{1}{2}-\frac{1}{2}} = \begin{pmatrix} 0 \\ 1 \end{pmatrix}. \tag{8}$$

The reduced radial part $g(r)$ of the upper component and $f(r)$ of the lower component of Dirac spinor $\psi_{nlj}(r)$ are the solutions of the equations given by

$$\frac{d^2g(r)}{dr^2} + \left[(E_D + m_q)[E_D - m_q - V(r)] - \frac{\kappa(\kappa+1)}{r^2}\right]g(r) = 0 \tag{9}$$

and

$$\frac{d^2f(r)}{dr^2} + \left[(E_D + m_q)[E_D - m_q - V(r)] - \frac{\kappa(\kappa-1)}{r^2}\right]f(r) = 0. \tag{10}$$

It can be transformed into a convenient dimensionless form given as [23]

$$\frac{d^2g(\rho)}{d\rho^2} + \left[\epsilon - \rho^{0.1} - \frac{\kappa(\kappa+1)}{\rho^2}\right]g(\rho) = 0 \tag{11}$$

and

$$\frac{d^2f(\rho)}{d\rho^2} + \left[\epsilon - \rho^{0.1} - \frac{\kappa(\kappa-1)}{\rho^2}\right]f(\rho) = 0. \tag{12}$$

In terms of dimensionless variable $\rho = (r/r_0)$ with the arbitrary scale factor chosen conveniently as

$$r_0 = \left[(m_q + E_D)\frac{\lambda}{2}\right]^{-\frac{10}{21}}, \tag{13}$$

and a corresponding dimensionless energy eigenvalue defined as

$$\epsilon = (E_D - m_q - V_0)(m_q + E_D)^{\frac{1}{21}}\left(\frac{2}{\lambda}\right)^{\frac{20}{21}}. \tag{14}$$

Here, it is suitable to define a quantum number κ by

$$\kappa = \begin{cases} -(l+1) = -(j+\frac{1}{2}) & \text{for } j = l+\frac{1}{2} \\ l = +(j+\frac{1}{2}) & \text{for } j = l-\frac{1}{2}. \end{cases} \tag{15}$$

Equations (11) and (12) now can be treated similar to the radial Schrödinger equation with a potential ρ^ν which can be solved numerically [24].

The solutions $g(\rho)$ and $f(\rho)$ are normalized to get

$$\int_0^\infty (f_q^2(r) + g_q^2(r))dr = 1. \tag{16}$$

The wave function for a $D_s(c\bar{s})$ meson now can be constructed using Eqs. (5) and (6) and the corresponding mass of the quark-antiquark system can be written as

$$M_{Q\bar{q}} = E_D^Q + E_D^{\bar{q}}, \tag{17}$$

where $E_D^{Q/\bar{q}}$ are obtained using Eqs. (14) and (15). For the spin triplet (vector) and spin singlet (pseudoscalar) state, the choices of $(j_1,\ j_2)$ are $((l_1+\frac{1}{2}),(l_1+\frac{1}{2}))$ and $((l_1+\frac{1}{2}),(l_1-\frac{1}{2}))$ respectively. The previous work of independent quark model within the Dirac formalism by [22] has been extended here by incorporating the spin-spin, spin-orbit and tensor interactions of the confined one-gluon exchange potential (COGEP) [25,26], in addition to the $j-j$ coupling of the quark-antiquark. Finally, the mass of the specific $^{2S+1}L_J$ states of the $Q\bar{q}$ system is expressed as

$$M_{^{2S+1}L_J} = M_{Q\bar{q}}(n_1 l_1 j_1, n_2 l_2 j_2) + \langle V_{Q\bar{q}}^{j_1 j_2}\rangle + \langle V_{Q\bar{q}}^{LS}\rangle + \langle V_{Q\bar{q}}^{T}\rangle. \tag{18}$$

The spin-spin part is defined here as

$$\langle V_{Q\bar{q}}^{j_1 j_2}(r)\rangle = \frac{\sigma\langle j_1 j_2 JM|\hat{j}_1\,\hat{j}_2\,|j_1 j_2 JM\rangle}{(E_Q + m_Q)(E_{\bar{q}} + m_{\bar{q}})}, \tag{19}$$

where σ is the $j-j$ coupling constant. The expectation value of $\langle j_1 j_2 JM|\hat{j}_1\,\hat{j}_2\,|j_1 j_2 JM\rangle$ contains the $(j_1 j_2)$ coupling and the square of Clebsch-Gordan coefficients. The tensor and spin-orbit parts of the confined one-gluon exchange potential (COGEP) [25,26] are given by

$$V_{Q\bar{q}}^T(r) = -\frac{\alpha_s}{4}\frac{N_Q^2 N_{\bar{q}}^2}{(E_Q + m_Q)(E_{\bar{q}} + m_{\bar{q}})} \otimes \lambda_Q\lambda_{\bar{q}}\left(\left(\frac{D_1''(r)}{3} - \frac{D_1'(r)}{3r}\right)S_{Q\bar{q}}\right), \tag{20}$$

where $S_{Q\bar{q}} = [3(\sigma_Q\hat{\vec{r}})(\sigma_{\bar{q}}\hat{\vec{r}}) - \sigma_Q\sigma_{\bar{q}}]$ and $\vec{\hat{r}} = \vec{\hat{r}}_Q - \vec{\hat{r}}_{\bar{q}}$ is the unit vector in the direction of $\vec{r}$ and

$$V_{Q\bar{q}}^{LS}(r) = \frac{\alpha_s}{4}\frac{N_Q^2 N_{\bar{q}}^2}{(E_Q + m_Q)(E_{\bar{q}} + m_{\bar{q}})}\frac{\lambda_Q\lambda_{\bar{q}}}{2r} \otimes [[r\times(\hat{p_Q} - \hat{p_q})(\sigma_Q + \sigma_q)](D_0'(r) + 2D_1'(r)) + [r\times(\hat{p_Q} + \hat{p_q})(\sigma_Q - \sigma_q)](D_0'(r) - D_1'(r))], \tag{21}$$

where α_s is the strong coupling constant and it is computed as

$$\alpha_s = \frac{4\pi}{(11 - \frac{2}{3}n_f)\log(\frac{E_Q^2}{\Lambda_{\rm QCD}^2})} \tag{22}$$

with $n_f = 3$ and $\Lambda_{\rm QCD} = 0.150$ GeV. In Eq. (21) the spin-orbit term has been split into symmetric $(\sigma_Q + \sigma_q)$ and antisymmetric $(\sigma_Q - \sigma_q)$ spin-orbit terms.

We have adopted the same parametric form of the confined gluon propagators which are given by [25,26]

$$D_0(r) = \left(\frac{\alpha_1}{r} + \alpha_2\right)\exp(-r^2c_0^2/2) \tag{23}$$

and

$$D_1(r) = \frac{\gamma}{r}\exp(-r^2c_1^2/2) \tag{24}$$

with $\alpha_1 = 0.036$, $\alpha_2 = 0.056$, $c_0 = 0.1017$ GeV, $c_1 = 0.1522$ GeV, $\gamma = 0.0139$. Other optimized model parameters employed in the present study are listed in Table I. The computed S-wave masses and other P-wave and D-wave masses of D_s meson states are listed in Tables II and III respectively. A statistical analysis of the sensitivity of the model parameters [i.e., potential strength

TABLE I. The fitted model parameters for the D_s systems.

System parameters	D_s
Quark mass (in GeV)	$m_s = 0.1$ and $m_c = 1.27$
Potential strength (λ)	$2.2655 + B$ GeV$^{\nu+1}$
V_0	-2.6155 GeV
Centrifugal parameter (B)	$(n*0.153)$ GeV^{-1} for $l=0$
	$((n+l)*0.1267)$ GeV^{-1} for $l\neq 0$
σ ($j-j$ coupling strength)	0.0055 GeV^3 for $l=0$
	0.2696 GeV^3 for $l\neq 0$

TABLE II. S-wave D_s $(c\bar{s})$ spectrum (in MeV).

						Experiment					
nL	J^P	State	$M_{Q\bar{q}}$	$\langle V^{j_1 j_2}_{Q\bar{q}} \rangle$	Present	Meson	Mass [1]	[27][a]	[28][b]	[15][c]	[29][d]
1S	1^-	1^3S_1	2113.2	0.73	2113.9	D_s^*	2112.3 ± 0.5		2111	2117	2107
	0^-	1^1S_0	1970.1	−1.84	1968.3	D_s	1968.49 ± 0.32		1969	1970	1969
2S	1^-	2^3S_1	2717.3	0.46	2717.8	$D_s^*(2710)$	2710^{+12}_{-7} [30,31]	2728	2731	2723	2714
	0^-	2^1S_0	2634.6	−1.06	2633.5	$D_s(2632)$	2632.5 ± 1.7 [3]	2656	2688	2684	2640
3S	1^-	3^3S_1	3263.5	0.33	3263.8			3200	3242	3180	
	0^-	3^1S_0	3203.2	−0.75	3202.4			3140	3219	3158	
4S	1^-	4^3S_1	3781.4	0.25	3781.6				3669	3571	
	0^-	4^1S_0	3732.7	−0.57	3732.1				3652	3556	

[a]Semirelativistic model.
[b]Quasipotential approach.
[c]Relativistic quark-antiquark potential (Coulomb plus power) model.
[d]Nonrelativistic constituent quark model.

(λ) and $j-j$ coupling strength σ in the present case] shows about 0.76% variations in the binding energy with 5% changes in the parameters λ and σ. Figure 1 shows the energy level diagram of D_s meson spectra along with available experimental results.

III. MAGNETIC (M1) TRANSITIONS OF OPEN CHARM MESON

Spectroscopic studies led us to compute the decay widths of energetically allowed radiative transitions of the type $A \to B + \gamma$ among several vector and pseudoscalar states of D_s meson. The magnetic transition corresponds to spin flip and hence the vector meson decay to pseudoscalar $V \to P\gamma$ represents a typical M1 transition. Such transitions are experimentally important to the identification of newly observed states. Assuming that such transitions are single vertex processes governed mainly by photon emission from independently confined quark and antiquark inside the meson, the S-matrix elements in the rest frame of the initial meson are written in the form

TABLE III. P-wave and D-wave D_s $(c\bar{s})$ spectrum (in MeV).

								Experiment					
nL	J^P	State	$M_{Q\bar{q}}$	$\langle V^{j_1 j_2}_{Q\bar{q}} \rangle$	$\langle V^T \rangle$	$\langle V^{LS} \rangle$	Present	Meson	Mass [1]	[27]	[28]	[15]	[29]
1P	2^+	1^3P_2	2520.9	19.24	−3.71	48.23	2584.7	$D_{s2}(2573)$	2571.9 ± 0.8		2571	2566	2559
	1^+	1^3P_1	2520.9	25.65	18.54	−48.23	2516.9	$D_{s1}(2536)$	2535.12 ± 0.13		2536	2540	2510
	0^+	1^3P_0	2520.9	−38.47	−37.08	−96.46	2349.0	$D_{s0}(2317)$	2317.8 ± 0.6		2509	2444	2344
	1^+	1^1P_1	2421.7	13.84	0	0	2435.6	$D_{s1}(2460)$	2459.6 ± 0.6		2574	2530	2488
2P	2^+	2^3P_2	3018.3	13.87	−6.28	81.75	3107.6			3045	3142	3048	3040
	1^+	2^3P_1	3018.3	18.50	31.40	−81.75	2986.4	$D_{sJ}(3040)$	3044^{+30}_{-9} [5]	3040	3067	3019	2958
	0^+	2^3P_0	3018.3	−27.75	−62.8	−163.51	2764.3			2970	3054	2947	2830
	1^+	2^1P_1	2949.4	9.64	0	0	2959.0			3020	3154	3023	2995
3P	2^+	3^3P_2	3479.7	10.76	−8.53	111.06	3593.0				3580		
	1^+	3^3P_1	3479.7	14.34	42.64	−111.06	3425.6				3519		
	0^+	3^3P_0	3479.7	−21.51	−85.27	−222.13	3150.9				3513		
	1^+	3^1P_1	3426.0	7.37	0	0	3433.4				3618		
1D	3^-	1^3D_3	2952.7	−21.79	−0.03	0.49	2931.4	$D_{sJ}^*(2860)$	2862^{+6}_{-3} [5]	2840	2971	2834	2811
	2^-	1^3D_2	2952.7	−64.74	0.11	−0.25	2887.8			2885	2961	2816	2788
	1^-	1^3D_1	2952.7	−109.81	−0.11	−0.75	2842.0			2870	2913	2873	2804
	2^-	1^1D_2	2874.3	−2.65	0	0	2871.6			2828	2931	2896	2849
2D	3^-	2^3D_3	3423.7	−15.72	−0.03	0.52	3408.4			3285	3469	3263	3240
	2^-	2^3D_2	3423.7	−46.71	0.11	−0.26	3376.8				3456	3248	3217
	1^-	2^3D_1	3423.7	−79.23	−0.11	−0.79	3343.5			3290	3383	3292	3217
	2^-	2^1D_2	3363.7	−1.87	0	0	3361.8				3403	3312	3260
3D	3^-	3^3D_3	3870.9	−12.06	−0.04	0.60	3859.4						
	2^-	3^3D_2	3870.9	−35.85	0.13	−0.30	3834.9						
	1^-	3^3D_1	3870.9	−60.80	−0.13	−0.91	3809.1						
	2^-	3^1D_2	3821.7	−1.42	0	0	3820.3						

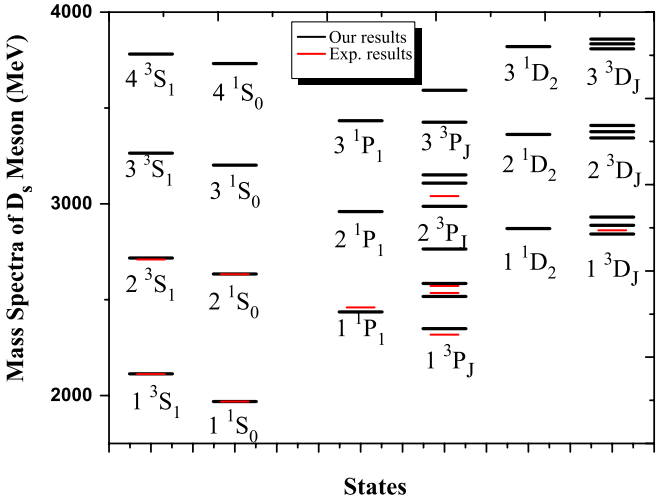

FIG. 1 (color online). D_s meson spectra.

$$S_{BA} = \left\langle B\gamma| - ie\int d^4xT\left[\sum_q e_q\bar{\psi}_q(x)\gamma^\mu\psi_q(x)A_\mu(x)\right]|A\right\rangle. \tag{25}$$

The common choice of the photon field $A_\mu(x)$ is made here in Coulomb gauge with $\epsilon(k,\lambda)$ as the polarization vector of the emitted photon having energy momentum $(k_0 = |\mathbf{k}|, \mathbf{k})$ in the rest frame of A. The quark field operators find possible expansions in terms of the complete set of positive and negative energy solutions given by Eqs. (5) and (6) in the form

$$\Psi_q(x) = \sum_\zeta [b_{q\zeta}\psi^{(+)}_{q\zeta}(r)\exp(-iE_{q\zeta}t) + b^\dagger_{q\zeta}\psi^{(-)}_{q\zeta}(r)\exp(iE_{q\zeta}t)], \tag{26}$$

where the subscript q stands for the quark flavor and ζ represents the set of Dirac quantum numbers. Here $b_{q\zeta}$ and $b^\dagger_{q\zeta}$ are the quark annihilation and the antiquark creation operators corresponding to the eigenmodes ζ. After some standard calculations (the details of calculations can be found in Refs. [32–34]), the S-matrix elements can be expressed as

$$S_{BA} = i\sqrt{\left(\frac{\alpha}{k}\right)}\delta(E_B + k - E_A)\sum_{q,m,m'}\langle B|[J^q_{m'm}(k,\lambda)b^\dagger_{qm'}b_{qm} - \tilde{J}^{\tilde{q}}_{mm'}(k,\lambda)\tilde{b}^\dagger_{qm'}\tilde{b}_{qm}]|A\rangle. \tag{27}$$

Here $E_A = M_A$, $E_B = \sqrt{k^2 + M_B^2}$ and (m, m') are the possible spin quantum numbers of the confined quarks corresponding to the ground state of the mesons. We have

$$J^q_{m'm}(k,\lambda) = e_q\int d^3r\exp(-i\vec{k}\,\vec{r})[\bar{\psi}_{qm'}(r)\vec{\gamma}\,\vec{\epsilon}(k,\lambda)\psi_{qm}(r)], \tag{28}$$

$$\tilde{J}^{\tilde{q}}_{mm'}(k,\lambda) = e_q\int d^3r\exp(-i\vec{k}\,\vec{r})[\bar{\phi}_{qm}(r)\vec{\gamma}\,\vec{\epsilon}(k,\lambda)\phi_{qm'}(r)]. \tag{29}$$

One can reduce the above equations to simple forms as

$$J^q_{m'm}(k,\lambda) = -i\mu_q(k)[\chi^\dagger_m(\vec{\sigma}\,\vec{K})\chi_m] \tag{30}$$

and

$$\tilde{J}^{\tilde{q}}_{mm'}(k,\lambda) = i\mu_q(k)[\tilde{\chi}^\dagger_m(\vec{\sigma}\,\vec{K})\tilde{\chi}_m], \tag{31}$$

where $\vec{K} = \vec{k}\times\vec{\epsilon}(k,\lambda)$. Equation (27) further simplified to get

$$S_{BA} = i\sqrt{\left(\frac{\alpha}{k}\right)}\delta(E_B + k - E_A) \times\sum_{q,m,m'}\langle B|\mu_q(k)[\chi^\dagger_{m'}\vec{\sigma}\,\vec{K}\,\chi_m b^\dagger_{qm'}b_{qm} + \tilde{\chi}^\dagger_m\vec{\sigma}\,\vec{K}\,\tilde{\chi}_{m'}\tilde{b}^\dagger_{qm'}\tilde{b}_{qm}]|A\rangle, \tag{32}$$

where $\mu_q(k)$ is expressed as

$$\mu_q(k) = \frac{2e_q}{k}\int_0^\infty j_1(kr)f_q(r)g_q(r)dr, \tag{33}$$

where $j_1(kr)$ is the spherical Bessel function and the energy of the outgoing photon in the case of a vector meson undergoing a radiative transition to its pseudoscalar state, for instance, $D_s^* \to D_s\gamma$ is given by

$$k = \frac{M^2_{D_s^*} - M^2_{D_s}}{2M_{D_s^*}}. \tag{34}$$

The relevant transition magnetic moment is expressed as

$$\mu_{D_s^*D_s}(k) = \frac{1}{3}[2\mu_c(k) - \mu_s(k)]. \tag{35}$$

Now, the magnetic (M1) transition width of $D_s^* \to D_s\gamma$ can be obtained as

$$\Gamma_{D_s^*\to D_s\gamma} = \frac{4\alpha}{3}k^3|\mu_{D_s^*D_s}(k)|^2. \tag{36}$$

The computed transition widths of low-lying S-wave states are tabulated in Table VI and are compared with other model predictions.

IV. DECAY CONSTANT OF D_S MESON

The decay constant of a meson is an important parameter in the study of leptonic or nonleptonic weak decay processes. The decay constant (f_p) of the pseudoscalar state is obtained by parametrizing the matrix elements of weak current between the corresponding meson and the vacuum as [35]

$$\langle 0|\bar{q}\gamma^{\mu}\gamma_5 c|P_{\mu}\rangle = if_p P^{\mu}. \tag{37}$$

It is possible to express the quark-antiquark eigenmodes in the ground state of the meson in terms of the corresponding momentum distribution amplitudes. Accordingly, eigenmodes, $\psi_A^{(+)}$ in the state of definite momentum p and spin projection s'_p can be expressed as

$$\psi_A^{(+)} = \sum_{s'_p} \int d^3p G_q(p, s'_p)\sqrt{\frac{m}{E_p}} U_q(p, s'_p)\exp(i\vec{p}\,\vec{r}), \tag{38}$$

where $U_q(p, s'_p)$ is the usual free Dirac spinors.

In the relativistic quark model, the decay constant can be expressed through the meson wave function $G_q(p)$ in the momentum space [33,36]

$$f_P = \left(\frac{3|I_p|^2}{2\pi^2 M_p J_p}\right)^{\frac{1}{2}}. \tag{39}$$

Here M_p is mass of the pseudoscalar meson and I_p and J_p are defined as

$$I_p = \int_0^{\infty} dp p^2 A(p)[G_{q1}(p)G^*_{q2}(-p)]^{\frac{1}{2}}, \tag{40}$$

$$J_p = \int_0^{\infty} dp p^2 [G_{q1}(p)G^*_{q2}(-p)], \tag{41}$$

respectively, where

$$A(p) = \frac{(E_{p1}+m_{q1})(E_{p2}+m_{q2})-p^2}{[E_{p1}E_{p2}(E_{p1}+m_{q1})(E_{p2}+m_{q2})]^{\frac{1}{2}}} \tag{42}$$

and $E_{p_i} = \sqrt{k_i^2 + m_{q_i}^2}$.

The computed decay constants of the D_s meson from $1S$ to $4S$ states are tabulated in Table VII. The present result for the $1S$ state is compared with experimental as well as other model predictions. There are no model predictions available for comparison of the decay constants of the $2S$ to $4S$ states.

V. LEPTONIC DECAY OF D_S MESON

Charged mesons produced from a quark and antiquark can decay to a charged lepton pair when these objects annihilate via a virtual $W^{\pm}$ boson as given in Fig. 2. Though the leptonic decays of open flavor mesons belong to rare decay [38,39], they have clear experimental signatures due to the presence of highly energetic leptons in the final state. Such decays are very clean due to the absence of hadrons in the final state [40]. The leptonic width of the D_s meson is computed using the relation given by

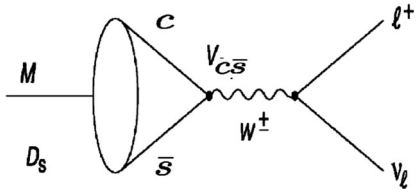

FIG. 2. Feynman diagram for leptonic decay ($M \to l\bar{\nu}_l$).

$$\Gamma(D_s^+ \to l^+\nu_l) = \frac{G_F^2}{8\pi} f_{D_s}^2 |V_{cs}|^2 m_l^2 \left(1 - \frac{m_l^2}{M_{D_s}^2}\right)^2 M_{D_s} \tag{43}$$

in complete analogy to $\pi^+ \to l^+\nu$. These transitions are helicity suppressed; i.e., the amplitude is proportional to m_l, the mass of the lepton l. The leptonic widths of the D_s (1^1S_0 state) meson are obtained from Eq. (43) where the predicted values of the pseudoscalar decay constant f_{D_s} along with the masses of M_{D_s} and the PDG value for $V_{cs} = 1.006$ are used. The leptonic widths for the separate lepton channel are computed for the choices of $m_{l=\tau,\mu,e}$. The branching ratio (BR) of these leptonic widths is then obtained as

$$\mathrm{BR} = \Gamma(D_s \to l^+\nu_l) \times \tau, \tag{44}$$

where τ is the experimental lifetime of the D_s meson. The respective leptonic widths are tabulated in Table VIII along with other model predictions as well as with the experimental values. Our results are found to be in accordance with the available experimental values.

VI. EXCLUSIVE SEMILEPTONIC AND HADRONIC DECAYS OF D_S MESON

The exclusive decays of heavy flavor hadrons play an important role in the determination of fundamental parameters of the electroweak standard model and in the development of a deeper understanding of QCD. Exclusive decays into few-body final states are often easier to measure, but the theory of exclusive processes is more demanding and hence still underdeveloped. The semileptonic and hadronic decays in exclusive modes are particularly important for testing the dynamics of heavy flavors. The Cabibbo favored semileptonic and hadronic decays of the D_s meson and their form factors are computed here. The form factors relevant to semileptonic and hadronic decays are related to the Isgur-Wise function $\xi(\omega)$ in heavy flavor symmetry.

The semileptonic decay of D_s meson is through $c \to ql^+\nu$, where $q = d, s$. The Cabibbo favored semileptonic decay widths $\Gamma(D_s \to \phi + l^+ + \nu_l)$ and $\Gamma(D_s \to K^0 + l^+ + \nu_l)$ are calculated using the expression given by [41]

$$\Gamma(D_s \to \phi + l^+ + \nu_l) = \frac{G_F^2 M_{D_s}^5}{768\pi^3}|V_{cs}|^2 f(x)|f_+^2(q^2)|, \tag{45}$$

$$\Gamma(D_s \to K^0 + l^+ + \nu_l) = \frac{G_F^2 M_{D_s}^5}{768\pi^3}|V_{cd}|^2 f(x)|f_+^2(q^2)|, \tag{46}$$

where $f(x)$ is the phase space correction [35] and is defined as $f(x) = 1 - 8x + 8x^3 - x^4 - 12x^2 \log x$, and x is expressed as, $x = (M_{(\phi,K^0)}/M_{D_s})^2$.

Studies of flavor changing decays of heavy flavor quarks are useful for determining the parameters of the standard model and for testing phenomenological models which include strong effects. The interpretation of the hadronic decays of c meson within a hadronic state is complicated by the effects of strong interaction and by its interplay with the weak interaction. The hadronic decays of heavy mesons can be understood in this model and we assume that Cabibbo favored hadronic decays proceed via the basic process ($c \to q + u + \bar{d}; q \in s, d$) and the decay widths are given by [35,42]

$$\Gamma(D_s \to \phi\pi^+) = C_f \frac{G_F^2|V_{cs}|^2|V_{ud}|^2 f_\pi^2}{32\pi M_{D_s}^3} \times [\lambda(M_{D_s}^2, M_\phi^2, M_\pi^2)]^{\frac{3}{2}}|f_+^2(q^2)| \tag{47}$$

for $q = s$ and

$$\Gamma(D_s \to K^0\pi^+) = C_f \frac{G_F^2|V_{cd}|^2|V_{ud}|^2 f_\pi^2}{32\pi M_{D_s}^3} \times [\lambda(M_{D_s}^2, M_{K^0}^2, M_\pi^2)]^{\frac{3}{2}}|f_+^2(q^2)| \tag{48}$$

for $q = d$. Here, C_f is the color factor and $(|V_{cs}|, |V_{cd}|, |V_{ud}|)$ are the Cabibbo-Kobayashi-Maskawa (CKM) mixing matrices. f_π is the decay constant of the π meson and its value is taken as 0.130 GeV. Here, $f_+(q^2)$ is the form factor and the factor $\lambda(M_{D_s}^2, M_{K^0}^2, M_\pi^2)$ can be computed as

$$\lambda(x, y, z) = x^2 + y^2 + z^2 - xy - yz - zx. \tag{49}$$

The renormalized color factor without the interference effect due to QCD is given by $(C_A^2 + C_B^2)$. The coefficients C_A and C_B are further expressed as [35]

$$C_A = \frac{1}{2}(C_+ + C_-), \tag{50}$$

$$C_B = \frac{1}{2}(C_+ - C_-), \tag{51}$$

where

$$C_+ = 1 - \frac{\alpha_s}{\pi}\log\left(\frac{M_W}{m_c}\right) \tag{52}$$

and

$$C_- = 1 + 2\frac{\alpha_s}{\pi}\log\left(\frac{M_W}{m_c}\right), \tag{53}$$

where M_W is the mass of W meson.

Consequently, the form factors $f_\pm(q^2)$ corresponding to the D_s final state are related to the Isgur-Wise function as [35]

$$f_\pm(q^2) = \xi(\omega)\frac{M_{D_s} \pm M_\phi}{2\sqrt{M_{D_s}M_\phi}}. \tag{54}$$

The Isgur-Wise function $\xi(\omega)$ can be evaluated according to the relation given by [42]

$$\xi(\omega) = \frac{2}{\omega - 1}\left\langle j_0\left(2E_q\sqrt{\frac{\omega - 1}{\omega + 1}}r\right)\right\rangle, \tag{55}$$

where E_q is the binding energy of decaying meson and ω is given by

$$\omega = \frac{M_{D_s}^2 + M_\phi^2 - q^2}{2M_{D_s}M_\phi}. \tag{56}$$

For a good approximation the form factor $f_-(q^2)$ does not contribute into the decay rate, so we have neglected it here. The heavy flavor symmetry provides model-independent normalization of the weak form factors $f_\pm(q^2)$ either at $q = 0$ or $q = q_{\max}$ and we have applied $q = q_{\max}$ in Eqs. (45) and (46) for exclusive semileptonic decay and $q = 0$ in Eqs. (47) and (48) for hadronic decay. From the computed exclusive semileptonic and hadronic decay widths, the branching ratios of the D_s meson are obtained from the relation

$$\mathrm{BR} = \Gamma \times \tau. \tag{57}$$

The lifetime of D_s ($\tau_{D_s} = 0.5$ ps^{-1}) is taken as the world average value reported by Particle Data Group (PDG-2012) [1]. The decay widths and their branching ratios are listed in Table IX along with the known experimental and other theoretical predictions for comparison.

TABLE IV. Comparison of center of mass in the D_s meson in MeV.

M_{CW}	Present	[37]	[28]	Experiment
$\overline{1S}$	2077.5	$2045.4 \pm 0.215 \pm 0.293$	2075.5	2076.3
$\overline{2S}$	2696.7		2720.2	2690.6
$\overline{3S}$	3248.4		3236.2	
$\overline{4S}$	3769.2		3664.7	
1^3P_J	2535.9		2552.4	2531.4
$\overline{1P}$	2510.8		2557.8	2513.4
2^3P_J	3029.0		3107.2	
$\overline{2P}$	3011.5		3118.9	

TABLE V. Mass splitting in D_s meson in MeV.

Splitting	Present	[37]	[28]	Experiment
$1^3S_1 - 1^1S_0$	145.6	$133.1 \pm 1.0 \pm 1.9$	143	143.8 ± 0.4
$2^3S_1 - 2^1S_0$	84.3	$72 \pm 24 \pm 1$	43	
$3^3S_1 - 3^1S_0$	61.4		23	
$4^3S_1 - 4^1S_0$	49.5		17	
$D_{s0}(2317)$-$\overline{1S}$	271.5	$341.2 \pm 7.7 \pm 4.8$	433.5	241.5 ± 0.8
$D_{s1}(2460)$-$\overline{1S}$	358.1	$459.8 \pm 6.4 \pm 6.4$	498.5	383.2 ± 0.8
$D_{s1}(2536)$-$\overline{1S}$	439.4	$494.6 \pm 9.2 \pm 6.9$	460.5	459.0 ± 0.5
$D_{s2}(2573)$-$\overline{1S}$	507.2	$536.7 \pm 9.2 \pm 7.5$	495.5	496.3 ± 1.0
$2^1S_0 - \overline{1S}$	556.0	$654.4 \pm 26.7 \pm 9.2$	612.5	
$2^3S_1 - \overline{1S}$	640.3	$726.4 \pm 20.8 \pm 10.2$	655.5	632.7^{+9}_{-6}

VII. RESULTS AND DISCUSSION

We have studied here the mass spectra and decay properties of the D_s meson in the framework of relativistic independent quark model. Our computed D_s meson spectral states are in good agreement with the reported PDG values of known states. Though there are many excited 1^- states of D_s meson known experimentally, most of them beyond $1S$ states are still not understood completely. In the case of P-wave states only 1^3P_J, 1^1P_1, and 2^1P_1 of the D_s meson are known experimentally. Our results are also compared with other theoretical model predictions.

The predicted masses of S-wave D_s meson state 2^3S_1 (2717.8 MeV) and 2^1S_0 (2633.5 MeV) are in very good agreement with the experimental result of 2710^{+12}_{-7} MeV by *BABAR* [30] and Belle [31] collaborations and 2638 MeV for 2^1S_0 by the SELEX collaboration [3], respectively. The expected results of other S-wave excited states of the D_s meson are also in good agreement with other reported values [15,27–29]. The predicted P-wave D_s meson states, 1^3P_2 (2584.7 MeV), 1^3P_1 (2516.9 MeV), 1^3P_0 (2349.0 MeV) and 1^1P_1 (2435.6 MeV), are in good agreement with experimental [1] results of 2571.9 ± 0.8 MeV, 2535.12 ± 0.13 MeV, 2317.8 ± 0.6 MeV and 2459.6 ± 0.6 MeV, respectively. The 2^3P_1 (2986.4 MeV) and $^3D_3$ (2931.4) are nearly 50–60 MeV off with the experimental results of 3044^{+30}_{-9} MeV [5] and 2862^{+6}_{-3} MeV [5]. However, their J^P values are not yet exactly confirmed. We consider them here as mixed states. Accordingly, D^*_{sJ} (2860) is found to be a mixed state of 1^3D_3 (2931.4) and 1^3D_1 (2842.0) with a mixing probability given by $\cos^2\theta = 0.2013$ and that for D_{sJ} (3040) as a mixed state of (1^3P_2 (3107.6) and 2^3P_0 (2764.3) with a mixing probability given by $\cos^2\theta = 0.8030$.

In the relativistic Dirac formalism, the spin degeneracy is primarily broken therefore, to have spin average masses of the different spectral states we employ the spin averaging procedure as

$$M_{CW} = \frac{\sum_J (2J+1) M_J}{\sum_J (2J+1)}. \tag{58}$$

The spin average or the center of weight masses M_{CW} are calculated from the known values of the different meson states and are compared with other model prediction [28] and those predicted by lattice QCD [LQCD] [37] in Table IV. It also helps us to know the different spin dependent contributions for the observed state.

The precise experimental measurements of the masses of D_s meson states provided a real test for the choice of the hyperfine and the fine structure interactions adopted in the study of D_s meson spectroscopy. Recent study of D_s meson mass splittings in lattice QCD [LQCD] [37] using 2 ± 1 flavor configurations generated with the Clover-Wilson fermion action by the PACS-CS collaboration [37] has been used for comparison. Present results as seen in Table V are in very good agreement with the respective experimental values over the lattice results [37]. In this Table, the present results on an average, are in agreement with the available experimental value within 6% of variations, while the lattice QCD predictions [37] show 20% of variations.

TABLE VI. Magnetic (M1) transition of open charm meson.

	k (MeV)		Γ (keV)					
Process	Present	[15]	Present	PDG [1]	[15]	[43]	[44]	[45]
$(1S)D^*_s \to D_s\gamma$	141.24	403	0.3443	< 4500	5.98	0.13	0.48	1.12
$(2S)D^*_s \to D_s\gamma$	83.48	152	0.0134		0.35			
$(3S)D^*_s \to D_s\gamma$	61.21	91	0.0030		0.08			
$(3S)D^*_s \to D_s\gamma$	49.47	65	0.0010		0.03			

TABLE VII. Pseudoscalar decay constant (f_P) of D_s systems (in MeV).

	f_P			
	1S	2S	3S	4S
Present	252.81	336.56	391.74	433.16
PDG [1]	260.0 ± 5.4			
Belle [46]	$255.5 \pm 4.2 \pm 5.1$			
BABAR [47]	$258.6 \pm 6.4 \pm 7.5$			
CLEO-c [48]	$259.0 \pm 6.2 \pm 3.0$			
CLEO-c [49]	$252.6 \pm 11.1 \pm 5.2$			
[*QCDSR*][a] [50]	246 ± 6			
[*RPM*][b] [51]	256 ± 26			
[*QCDSR*] [52]	245.3 ± 15.7			
[*LQCD*][c] [53]	244 ± 8			
[*LQCD*] [54,55]	248.0 ± 2.5			
[*LQCD*] [56]	260.1 ± 10.8			
[*LFQM*][d] [57]	264.5 ± 17.5			
[*QCDSR*] [58]	241 ± 12			
[*RBSM*][e] [20]	248 ± 27			

[a]QCD sum rule.
[b]Relativistic potential model.
[c]Lattice QCD.
[d]Light front quark model.
[e]Relativistic Bethe-Salpeter method.

The magnetic transitions (M1) can probe the internal charge structure of hadrons, and therefore they will likely play an important role in determining the hadronic structures of the D_s meson. The present M1 transition widths of D_s meson states as listed in Table VI are in accordance with the model prediction of [44] while the upper bound provided by PDG [1] is very wide. We do not find any theoretical predictions for M1 transition width of excited states for comparison. Thus we only look forward to see future experimental support to our predictions.

The calculated pseudoscalar decay constant (f_P) of the D_s meson is listed in Table VII along with other model predictions as well as experimental results. The value of $f_{D_s}(1S) = 252.81$ MeV obtained in our present study is in very good agreement with the experimental values provided by Belle [46], *BABAR* [47] and CLEO-c [48,49]. The present value is also in accordance with other theoretical predictions for the $1S$ state. The predicted f_{D_s} for higher S-wave states are found to increase with energy. However, there are no experimental or theoretical values available for comparison. Another important property of D_s meson studied in the present case is the leptonic decay widths. The present branching ratios for $D_s \to \tau\bar{\nu}_\tau$ (5.706×10^{-2}) and $D_s \to \mu\bar{\nu}_\mu$ (5.812×10^{-3}) are in excellent agreement with the experimental results $(5.43 \pm 0.31) \times 10^{-2}$ and $(5.90 \pm 0.33) \times 10^{-3}$ respectively over other theoretical predictions vide Table VIII. Large experimental uncertainty in the electron channel make it difficult for any reasonable conclusion.

The Cabibbo favored semileptonic branching ratios $\mathrm{BR}(D_s \to \phi e^+\nu_e)$ and $\mathrm{BR}(D_s \to \phi\pi^+)$ obtained respectively as 2.01% and 4.62% listed in Table IX are in very good agreement with PDG values of $2.49 \pm 0.14\%$ and $4.5 \pm 0.4\%$ respectively. The $\mathrm{BR}(D_s \to K^0\pi^+), 2.16 \times 10^{-3}$ is also in good accord with the branching ratio of $2.40 \pm 0.18 \times 10^{-3}$ reported by Belle collaboration [60]. While $\mathrm{BR}(D_s \to K^0 e^+\nu_e), 6.6 \times 10^{-3}$ is about 30% off with respect to the experimental [1] value of 3.7×10^{-3}. However, by incorporating the first order QCD correction to the phase space factor $f(x)$ as [35] $f(x) \to (f(x) - \frac{\alpha_s}{\pi} g(x))$ in Eq. (46), we obtained the BR $(D_s \to K^0 e^+\nu_e)$, 4.05×10^{-3} which is comparable with the PDG value of $(3.7 \pm 1.0) \times 10^{-3}$.

Finally we look forward to see future experimental support in favor of many of our predictions on the spectral states and decay properties of the open charm-strange meson. We would also like to extend the present scheme to study other heavy flavor hadrons.

TABLE VIII. The leptonic decay width and leptonic branching ratio (BR) of the D_s meson.

	$\Gamma(D_s \to l\bar{\nu}_l)$ (keV)		BR			
Process	Present	[36]	Present	[15]	[36]	Experiment [1]
$D_s \to \tau\bar{\nu}_\tau$	7.508×10^{-8}	6.090×10^{-8}	5.706×10^{-2}	4.22×10^{-2}	4.3×10^{-2}	$(5.43 \pm 0.31) \times 10^{-2}$
$D_s \to \mu\bar{\nu}_\mu$	7.648×10^{-9}	6.240×10^{-9}	5.812×10^{-3}	4.25×10^{-3}	4.41×10^{-3}	$(5.90 \pm 0.33) \times 10^{-3}$
$D_s \to e\bar{\nu}_e$	1.792×10^{-13}		1.362×10^{-7}	1.00×10^{-7}		$< 1.2 \times 10^{-4}$

TABLE IX. The exclusive semileptonic and hadronic decay width and branching ratio (BR) of the D_s meson.

	$\Gamma(D_s)$ (keV)	BR		
Process	Present	Present	[59]	Experiment [1]
$D_s \to \phi e^+\nu_e$	2.646×10^{-8}	2.01%		$(2.49 \pm 0.14)\%$
$D_s \to K^0 e^+\nu_e$	8.694×10^{-9}	6.60×10^{-3}		$(3.7 \pm 1.0) \times 10^{-3}$
$D_s \to \phi\pi^+$	4.724×10^{-8}	4.62%	4.38 ± 0.35	$(4.5 \pm 0.4)\%$
$D_s \to K^0\pi^+$	2.216×10^{-9}	2.16×10^{-3}	$(2.73 \pm 0.26) \times 10^{-3}$	$(2.40 \pm 0.18) \times 10^{-3}$ [60]

ACKNOWLEDGMENTS

This work is part of Major Research Project No. F. 40-457/2011(SR) funded by UGC, India. One of the authors (Bhavin Patel) acknowledges the support through the Fast Track project funded by DST (SR/FTP/PS-52/2011).

[1] J. Beringer *et al.* (Particle Data Group), Phys. Rev. D **86**, 010001 (2012).
[2] Q. Wanga, C. Hanhart, and Q. Zhao, arXiv:1311.2401v1.
[3] A. V. Evdokimov *et al.* (SELEX Collaboration), Phys. Rev. Lett. **93**, 242001 (2004).
[4] J. Brodzicka *et al.* (Belle Collaboration), Phys. Rev. Lett. **100**, 092001 (2008).
[5] B. Aubert *et al.* (*BABAR* Collaboration), Phys. Rev. D **80**, 092003 (2009).
[6] S. Godfrey and N. Isgur, Phys. Rev. D **32**, 189 (1985).
[7] S. Godfrey and R. Kokoski, Phys. Rev. D **43**, 1679 (1991).
[8] M. Di Pierro and E. Eichten, Phys. Rev. D **64**, 114004 (2001).
[9] D. Ebert, R. N. Faustov, and V. O. Galkin, Phys. Rev. D **67**, 014027 (2003).
[10] W. A. Bardeen, E. J. Eichen, and C. T. Hill, Phys. Rev. D **68**, 054024 (2003).
[11] P. Colangelo, F. De Fazio, and R. Ferrandes, Nucl. Phys. B, Proc. Suppl. **163**, 177 (2007).
[12] A. F. Falk and T. Mehen, Phys. Rev. D **53**, 231 (1996).
[13] E. J. Eichen, C. T. Hill, and C. Quigg, Phys. Rev. Lett. **71**, 4116 (1993).
[14] Bhavin Patel and P. C. Vinodkumar, Chin. Phys. C **34**, 1497 (2010); arXiv:0908.2212v1.
[15] N. Devlani and A. K. Rai, Phys. Rev. D **84**, 074030 (2011).
[16] A. K. Rai, B. Patel, and P. C. Vinodkumar, Phys. Rev. C **78**, 055202 (2008).
[17] D. Ebert, R. N. Faustov, and V. O. Galkin, Mod. Phys. Lett. A **18**, 601 (2003).
[18] J. P. Lansberg and T. N. Pham, Phys. Rev. D **74**, 034001 (2006); **75**, 017501 (2007); arXiv:0804.2180v1.
[19] C. S. Kim, T. Lee, and G. L. Wang, Phys. Lett. B **606**, 323 (2005); arXiv:hep-ph/0411075.
[20] G. L. Wang, Phys. Lett. B **633**, 492 (2006).
[21] G. Cvetic, C. Kim, G.-L. Wang, and W. Namgung, Phys. Lett. B **596**, 84 (2004).
[22] N. Barik, B. K. Dash, and M. Das, Phys. Rev. D **31**, 1652 (1985).
[23] N. Barik and S. N. Jena, Phys. Rev. D **26**, 2420 (1982).
[24] B. Patel and P. C. Vinodkumar, J. Phys. G **36**, 035003 (2009).
[25] P. C. Vinodkumar, K. B. Vijaya Kumar, and S. B. Khadkikar, Pramana J. Phys. **39**, 47 (1992).
[26] S. B. Khadkikar and K. B. Vijaya Kumar, Phys. Lett. B **254**, 320 (1991).
[27] A. M. Badalian and B. L. G. Bakker, Phys. Rev. D **84**, 034006 (2011).
[28] D. Ebert, R. N. Faustov, and V. O. Galkin, Eur. Phys. J. C **66**, 197 (2010).
[29] D.-M. Li, P.-F. Ji, and B. Ma, Eur. Phys. J. C **71**, 1582 (2011).
[30] J. Brodzicka *et al.* (Belle Collaboration), Phys. Rev. Lett. **100**, 092001 (2008).
[31] B. Aubert *et al.* (*BABAR* Collaboration), Phys. Rev. Lett. **97**, 222001 (2006).
[32] N. Barik, P. C. Dash, and A. R. Panda, Phys. Rev. D **46**, 3856 (1992).
[33] N. Barik, P. C. Dash, and A. R. Panda, Phys. Rev. D **47**, 1001 (1993).
[34] S. N. Jena, S. Panda, and T. C. Tripathy, Nucl. Phys. **A658**, 249 (1999).
[35] Q. Ho-Kim and P. Xuan-Yem, *The Particles and their Interactions: Concept and Phenomena* (Spinger-Verlag, Berlin, 1998).
[36] H. Ç. Iftci, and H. Koru, Int. J. Mod. Phys. E **09**, 407 (2000).
[37] D. Mohler and R. M. Woloshyn, Phys. Rev. D **84**, 054505 (2011).
[38] K. Hikasa *et al.* (Particle Data Group), Phys. Rev. D **45**, S1 (1992).
[39] J. L. Rosner and S. Stone, arXiv:0802.1043v1.
[40] S. Villa, Review of Bu Leptonic Decays, Bled, 2007, econf C070512, 014 (2007).
[41] Fayyazuddin and Riazuddin, *A Modern Introduction to Particle Physics* (World Scientific Publishing, Singapore, 1992).
[42] M. G. Olsson and S. Veseli, Phys. Rev. D **51**, 2224 (1995).
[43] S. N. Jena, S. Panda, and J. N. Mohanty, J. Phys. G **24**, 1869 (1998).
[44] H. Ç. Iftci, and H. Koru, Mod. Phys. Lett. A **16**, 1785 (2001).
[45] S. F. Radford, W. W. Repko, and M. J. Saelim, Phys. Rev. D **80**, 034012 (2009).
[46] A. Zupanc *et al.* (Belle Collaboration), J. High Energy Phys. 09 (2013) 139.
[47] P. del Amo Sanchez *et al.* (*BABAR* Collaboration), Phys. Rev. D **82**, 091103 (2010).
[48] P. Naik *et al.* (CLEO Collaboration), Phys. Rev. D **80**, 112004 (2009).
[49] P. U. E. Onyisi *et al.* (CLEO Collaboration), Phys. Rev. D **79**, 052002 (2009).
[50] S. Narison, Phys. Lett. B **718**, 1321 (2013).
[51] M.-Z. Yang, Eur. Phys. J. C **72**, 1880 (2012).
[52] W. Lucha, D. Melikhov, and S. Simula, Phys. Lett. B **701**, 82 (2011).
[53] B. Blossier *et al.*, J. High Energy Phys. 07 (2009) 043.
[54] C. T. H. Davies, C. McNeile, E. Follana, G. P. Lepage, H. Na, and J. Shigemitsu (HPQCD Collaboration), Phys. Rev. D **82**, 114504 (2010).

[55] H. Na, C. J. Monahan, C. T. H. Davies, R. Horgan, G. Peter Lepage, and J. Shigemitsu (HPQCD Collaboration), Phys. Rev. D **86**, 034506 (2012).
[56] A. Bazavov *et al.*, Phys. Rev. D **85**, 114506 (2012).
[57] C. W. Hwang, Phys. Rev. D **81**, 114024 (2010).
[58] Z.-G. Wang, J. High Energy Phys. 10 (2013) 208.
[59] H.-Y. Cheng and C.-W. Chiang, Phys. Rev. D **81**, 074021 (2010).
[60] E. Won, B. R. Ko *et al.* (Belle Collaboration), Phys. Rev. D **80**, 111101 (2009).